Enhancing UV photoconductivity of ZnO nanobelt by polyacrylonitrile functionalization

J. H. He,[a),b)] Yen H. Lin, Michael E. McConney, Vladimir V. Tsukruk, and Zhong L. Wang[a),c)]
School of Materials Science and Engineering, Georgia Institute of Technology, Atlanta, Georgia 30332-0245, USA

Gang Bao[a),d)]
School of Biomedical Engineering, Georgia Institute of Technology, , Atlanta, Georgia 30332, USA and Emory University, Atlanta, Georgia 30332, USA

(Received 26 June 2007; accepted 21 August 2007; published online 18 October 2007)

UV photodetector fabricated using a single ZnO nanobelt (NB) has shown a photoresponse enhancement up to 750 times higher than that of a bare ZnO NB after coating with ~20 nm plasma polymerized acrylonitrile (PP-AN) nanoscale film. The mechanism for this colossal photoconductivity is suggested as a consequence of the efficient exciton dissociation under UV illumination due to enhanced electron transfer from valence band of ZnO NB to the PP-AN and then back to the conduction band of ZnO. This process has demonstrated an easy and effective method for improving the performance of the nanowire/NB-based devices, possibly leading to supersensitive UV detector for applications in imaging, photosensing, and intrachip optical interconnects. © *2007 American Institute of Physics*. [DOI: 10.1063/1.2798390]

INTRODUCTION

Integrating nanophotonics with nanoelectronics is essential for developing the technologies for the next generation communication, computing, and biomedical imaging. Low-dimensional nanostructures, such as nanodots,[1] nanotubes,[2] and nanowires (NWs),[3–6] have been extensively studied for high sensitive optical detection, among which ZnO is a typical example.

ZnO exhibits the most diverse and abundant configurations of nanostructures known so far, such as hierarchical nanostructures,[7] NWs,[6] nanobelts (NBs),[8] nanosprings,[9] nanorings,[10] nanobows,[11] and nanohelices.[12] Due to semiconducting and piezoelectric properties of ZnO, numerous studies have demonstrated potential applications in electronics and optoelectronics based on ZnO nanostructures, such as optically pumped nanolaser,[6] nanogenerator,[13] acoustic resonator,[14] piezoelectric gated diode,[15] field emitter,[16] photodiode,[17] and photoconductor.[18,19]

Since the large surface-to-volume ratio of one-dimensional ZnO nanostructures and the presence of deep level surface trap state in NWs/NBs, ZnO exhibits long lifetime photocarriers,[18–22] and it usually exhibits lower photosensitivity than photodiodes.[23,24] To date, despite a great deal of research on the photosensing using nanowires, only a few of them reporting the improvement of photoresponse of NWs/NBs-based photoconductor.[25]

In this work, we present a bilayer polymer/ZnO photoconductor based on ZnO NBs and plasma polymerized acrylonitrile (PP-AN) nanoscale surface coating. By taking advantage of a rectangular cross section of NBs, uniform bilayered PP-AN/ZnO NBs were fabricated by exploiting plasma enhanced chemical vapor deposition (PECVD). We demonstrated that under identical UV illumination conditions, the photocurrent of ZnO NBs was increased by a factor of 750 after coating with PP-AN. The suggested mechanism includes a consequence of the efficient exciton dissociation under UV illumination due to enhanced electron transfer from valence band of ZnO NB to the photon-excited PP-AN rich on double and triple carbon-nitrogen bonds and then back to the conduction band of ZnO. The present study on the PP-AN-functionalized NBs presents a simple and cost-effective method for improving the performance of oxide NW/NB-based devices, possibly leading to a new generation of potential photodetector for applications such as imaging, photosensing, and intrachip optical interconnects.

EXPERIMENTS

In catalytically activated vapor phase transport and condensation deposition process, a 2-nm-thick Au thin film was deposited onto (11–20) Al_2O_3 substrate surface at room temperature using an electron beam evaporation system (~5×10^{-6} Torr), and Au serves as the catalyst for the growth. The experimental apparatus includes a horizontal tube furnace, a rotary pump system, and a gas supply system. A mixture of commercial ZnO and graphite powders in a ratio of Zn:C=4:1 was placed in an alumina boat, which was heated to a peak temperature of 1100 °C. The Al_2O_3 substrate was placed at a temperature zone of ~700 °C for collecting ZnO nanostructures. After the tube had been evacuated to a pressure of 1×10^{-3} Torr, the mixed sources at high-temperature zone was heated to 1100 °C at a rate of 5 °C/min and held at 1100 °C for 60 min with a carrier gas of $Ar+O_2$ flowing through the tube. Morphological studies of grown ZnO nanostructures have been performed with a LEO 1530 field emission scanning electron microscopy (SEM). A representative SEM image of the grown ZnO NBs is shown in Fig. 1(a). After the growth process, the substrate-

[a)]Authors to whom correspondence should be addressed.
[b)]Electronic mail: jhhe@cc.ee.ntu.edu.tw
[c)]Electronic mail: zhong.wang@mse.gatech.edu
[d)]Electronic mail: gang.bao@bme.gatech.edu

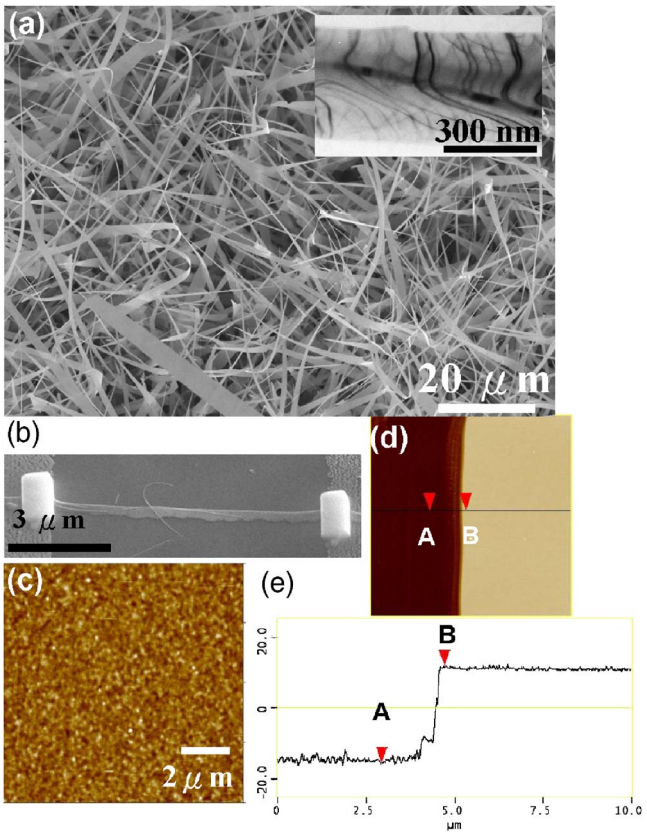

FIG. 1. (Color online) (a) A representative SEM image of ZnO nanobelts. The inset is a TEM image of a ZnO nanobelt. (b) The SEM image of a single ZnO NB device. (c) AFM topographic image of plasma-polymerized acrylonitrile (PP-AN) (z scale is 10 nm, roughness is 0.7 nm). (d) AFM image for scratching test. The left-hand side film is PP-AN. (e) AFM line profile analysis of coated film thickness. Note that A and B in (d) correspond to A and B in (e).

bound NBs were mechanically scrapped and sonicated in ethanol and deposited on carbon-coated copper grids for transmission electron microscopy (TEM) characterization. The inset in Fig. 1(a) is a TEM image, which indicates that ZnO NBs is single crystalline and free of dislocations. The synthesized ZnO nanobelts are transferred from the Al_2O_3 substrate to prepatterned Au/Ti electrodes by touching the NB sample with the electrodes. A single ZnO NB device lying across two electrodes could be achieved easily using this method. To reduce the contact resistance, focused ion beam (FIB) microscopy is employed to deposit conducting mixture of Pt on the contacts between ZnO and Au/Ti electrodes. The prepatterned Au/Ti electrodes for contacting probes of current-voltage (I-V) measurements were fabricated on 100 nm Si_3N_4/Si wafer through a typical process in the literature.[26] The electrode pattern was designed to have a few parallel electrodes separated by 5–20 μm. After the ZnO NB device fabrication, the PP-AN was deposited as a nanoscale surface layer by using PECVD technology with argon (50–200 cm^3/min, 99.999%) as the carrier gas within a custom built chamber according to the procedure published elsewhere.[27] The oxygen plasma treatment was carried out for eliminating the surface contamination of ZnO NB device before depositing PP-AN using PECVD. Figure 1(b) is a representative SEM image of a single ZnO NB device. Figure 1(c) shows topographic atom force microscopy (AFM, Dimension 3000, Digital Instruments) image of highly cross-linked PECVD PP-AN surface. The microroughness of the PP-AN was less than 0.7 nm (within 5×5 μm^2 area), indicating a smooth and uniform surface morphology with a fine, granular nanodomain texture, which is a typical surface morphology of plasma polymerized polymers with high cross-linking density.[28] The average thickness of the PP-AN coating 20 nm was obtained from the AFM scratch test [Figs. 1(d) and 1(e)] and confirmed with ellipsometry.

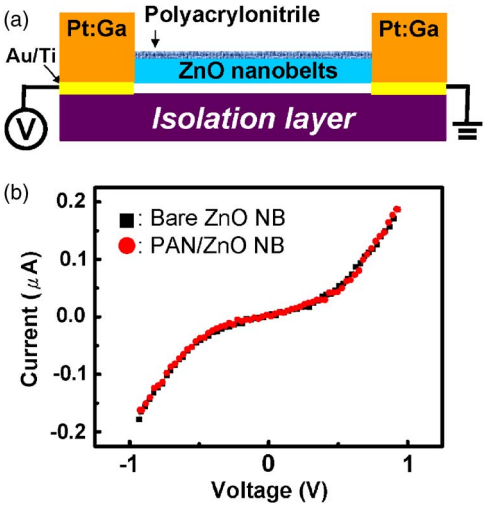

FIG. 2. (Color online) (a) The schematic diagram of PP-AN/ZnO NB device. (b) The I-V characteristic of a bare ZnO NB device and a PP-AN/ZnO NB device.

RESULTS AND DISCUSSION

Figure 2(a) shows the resultant schematic structure of PP-AN/ZnO NB device. The electron transport of a single ZnO NB was then studied. Figure 2(b) indicates the I-V characteristic of a bare ZnO NB device and a PP-AN/ZnO NB device. The device shows an almost identical I-V characteristic before and after depositing the PP-AN on ZnO NBs, and there is no change in the current transported through the NB, suggesting that the coated PP-AN has a much lower conductivity than that of ZnO. In fact, PP-AN is known as an insulating polymer with ultrahigh electrical resistivity.[27] Therefore, the total conductance of the PP-AN/ZnO NB is the conductance of the ZnO NB alone.

To further explore the performance, we compared the photocurrent of the ZnO before and after PP-AN coating under identical UV illumination condition. The UV light source used in the experiment is a 100 W UV lamp with a wavelength of 365 nm which is above the band gap of ZnO. All samples performed in the experiments of photoresponse were carried out under identical measurement conditions (e.g., position of UV light source and the distance between light source and measured samples). Both the bare ZnO NB and the PP-AN/ZnO NB photoconductors showed an on/off state corresponding to the exposure of the UV light, as shown in Fig. 3. Figure 3(a) is an intrinsic photoresponse of the bare ZnO NB under UV illumination. The current flowing through the bare ZnO NB increased with a ~12% en-

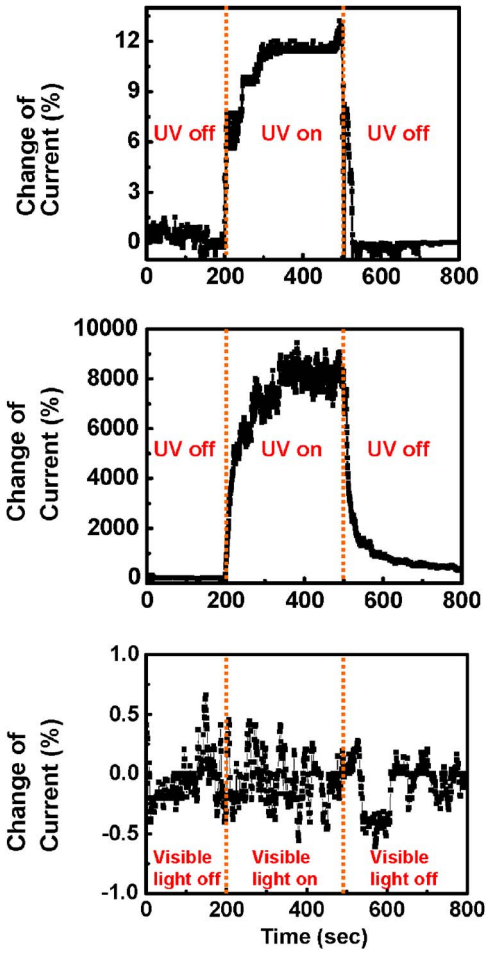

FIG. 3. (Color online) Photocurrent of (a) a bare ZnO NB device and (b) a PP-AN/ZnO NB device under UV light illumination, received under identical measurement conditions. (c) Photocurrent of PP-AN/ZnO NB device under visible light illumination. Note that vertical axis is the ratio of the photocurrent to dark current. The photocurrent was derived by subtracting dark current from the observed total current.

hancement upon the exposure of the UV light. Here, the enhancement is the photocurrent-to-dark-current ratio. The photocurrent is deduced by subtracting the dark current from the current measured under UV. Surprisingly, for the PP-AN/ZnO NB, the photocurrent increased up to ~9000%, as shown in Fig. 3(b), a huge increase by a factor of 750 times in comparison with that of bare ZnO NB (~12%). Turning UV light off resulting in fast decrease of the photocurrent to the background level and overall cycling in photocurrent intensity was reproducible for many on-off cycles. Therefore, functionalizing the ZnO NBs by a thin layer of PP-AN is an effective and cost-effective approach for enhancing the optical response of NBs for UV detection.

In contrast, by replacing UV with visible light, the photoresponse of PP-AN/ZnO shows no enhancement at all [Fig. 3(c)]. The absence of photoconduction upon visible light illumination indicates the absence of defect states,[18–20] such as oxygen vacancies in the PP-AN/ZnO NBs, indicating that there is no detectable level of defects created in the NB after PP-AN coating.

To clarify the mechanism of ultrahigh photoresponse of PP-AN/ZnO NB photodetectors, the PP-AN film alone was

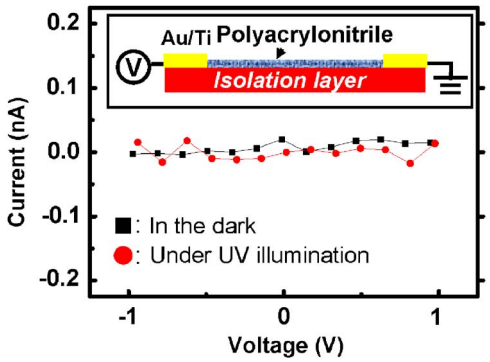

FIG. 4. (Color online) *I-V* measurements of PP-AN films in the dark and under UV illumination. The inset is a schematic diagram of the measurement.

examined by electrical and fluorescence (FL) measurements. First, PP-AN films were deposited between the two parallel electrodes separated by 5–20 μm. *I-V* measurements in the dark and under UV illumination were performed, as shown in Fig. 4. The inset in Fig. 4 is a schematic diagram of the measurement for PP-AN films. PP-AN shows the insulating electrical property and absence of photoconduction under UV illumination, which indicates no distinctive change of conductivity under UV illumination. The emission spectrum of PP-AN is shown in Fig. 5, which exhibited a broad peak at the wavelength of around 550 nm. The photoluminescence of PP-AN is associated with the π-π^* electronic transition in C═N and C≡N groups in PP-AN,[29,30] with the presence of these groups in highly cross-linked material confirmed by Fourier transform infrared spectroscopy and x-ray photoelectron spectroscopy studies as reported elsewhere.[31] In fact, the

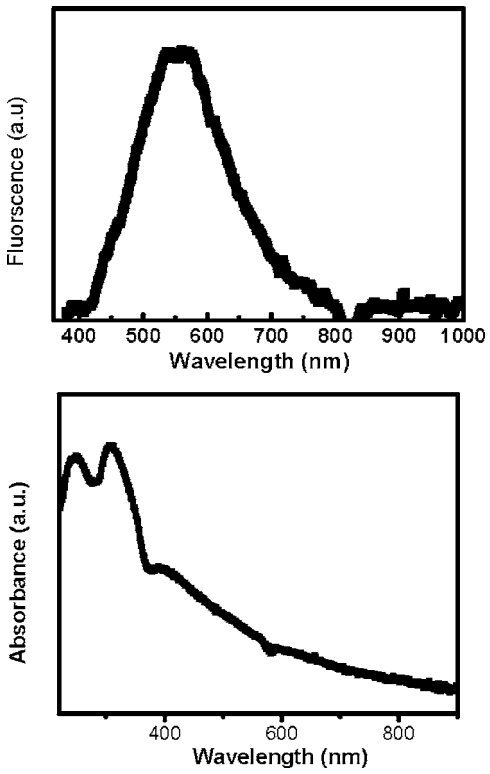

FIG. 5. Fluorescence (top) and UV (bottom) spectra of a PP-AN coating.

UV-visible spectroscopy confirmed the presence of strong absorption bands around 250 and 310 nm attributed to the π-π^* electronic transition of the nitrile group and the C $\equiv$N Π absorption.[30,32,33] These peaks with the appearance of a broad absorbance at higher wavelength reflect the formation of C=N π electron conjugation system for the plasma polymers indicating an extended conjugated π system in highly cross-linked PP-AN.[32]

Generally, the molecular structures of plasma polymerized molecular are different from starting monomers, because the polymers are formed with highly decomposed molecules under ions and electron reactions with high energy.[34] Moreover, the shift of peak in the photoluminescence (PL) associated with the morphology transition could be explained in terms of the rearrangement of intermolecular structure in the polymer backbone as the size and dimensionality of PP-AN nanomaterials change.[28,35] The emission spectrum of PP-AN means that electrons in the PP-AN were excited to a higher energy state (excited state) under the exposure of UV light, which left an unoccupied orbital (ground state) at an energy level that falls within the band gap of ZnO. At the same time, the electrons inside the ZnO NB were also excited under the exposure of the UV illumination. The ground state and excited state of PP-AN acted as a transition state for the electron in the valance band of ZnO to transit to the conduction band of ZnO. This hopping process of electrons from the valance band of ZnO to PP-AN and then back to the conduction band of ZnO is suggested to be responsible for the much enhanced conductivity of the PP-AN/NB device.

CONCLUSION

In summary, we have explored the photoconduction of an inorganic-organic hybrid NB. A simple coating of PP-AN on the ZnO NB increased its photoconductivity by a factor of 750 times in comparison with that of a bare ZnO NB. This effect is suggested as a consequence of the high efficiency of exciton dissociation under UV illumination due to efficient electron transfer from valence band of ZnO NB to the PP-AN and then back to the conduction band of ZnO. Emission spectrum of the PP-AN films shows good agreement with the exciton dissociation model that is electron excited from the ground state to the excited state. The present study on the PP-AN-functionalized NBs presents a simple and cost-effective method for improving the performance of oxide NW/NB-based devices for photodetection, possibly leading to a motivation for studying the optoelectronic properties of inorganic-organic hybrid nanomaterials. In order to gain more insight into the prospects of inorganic-organic hybrid photodector, the measurements that have been demonstrated here could form the basis of future, more detailed studies, such as the responsivity and quantum efficiency of the polymer-coated ZnO nanostructure photodetector. In addition, the dynamical response in comparison with conventional UV detectors needs to be discussed further due to the possible trapping processes at interface and/or surface states.

ACKNOWLEDGMENTS

This work was supported in part by the National Heart Lung and Blood Institute of the NIH as a Program of Excellence in Nanotechnology (1U01HL80711 to G.B.) and by the National Cancer Institute of the NIH as a Center of Cancer Nanotechnology Excellence (5U54CA119338 to G.B. and Z.L.W.). The authors thank T. J. Bunning, H. Jiang, and J. O. Enlow (AFRL) for technical assistance.

[1] V. L. Colvin, M. C. Schlamp, and A. P. Alivisatos, Nature (London) **370**, 354 (1994).
[2] J. A. Misewich, R. Martel, P. Avouris, J. C. Tsang, S. Heinze, and J. Tersoff, Science **300**, 783 (2003).
[3] X. Duan, Y. Huang, R. Agarwal, and C. M. Lieber, Nature (London) **421**, 241 (2003).
[4] J. H. He, R. S. Yang, Y. L. Chueh, L. J. Chou, L. J. Chen, and Z. L. Wang, Adv. Mater. (Weinheim, Ger.) **18**, 650 (2006).
[5] J. H. He, T. H. Wu, C. L. Hsin, K. M. Li, L. J. Chen, Y. L. Chueh, L. J. Chou, and Z. L. Wang, Small **2**, 116 (2006).
[6] M. H. Huang, S. Mao, H. Feick, H. Q. Yan, Y. Y. Wu, H. Kind, E. Weber, R. Russo, and P. D. Yang, Science **292**, 1897 (2001).
[7] J. Y. Lao, J. G. Wen, and Z. F. Ren, Nano Lett. **2**, 1287 (2002).
[8] Z. W. Pan, Z. R. Dai, and Z. L. Wang, Science **291**, 1947 (2001).
[9] X. Y. Kong and Z. L. Wang, Nano Lett. **3**, 1625 (2003).
[10] X. Y. Kong, Y. Ding, R. Yang, and Z. L. Wang, Science **303**, 1348 (2004).
[11] W. L. Hughes and Z. L. Wang, J. Am. Chem. Soc. **126**, 6703 (2004).
[12] P. X. Gao, Y. Ding, W. J. Mai, W. L. Hughes, C. S. Lao, and Z. L. Wang, Science **309**, 1700 (2005).
[13] Z. L. Wang and J. H. Song, Science **312**, 242 (2006).
[14] B. A. Buchine, W. L. Hughes, F. L. Degertekin, and Z. L. Wang, Nano Lett. **6**, 1155 (2006).
[15] H. He, C. L. Hsin, J. Liu, L. J. Chen, and Z. L. Wang, Adv. Mater. (Weinheim, Ger.) **19**, 781 (2007).
[16] Y. B. Li, Y. Bando, and D. Golberg, Appl. Phys. Lett. **84**, 3603 (2004).
[17] J. H. He, S. T. Ho, T. B. Wu, L. J. Chen, and Z. L. Wang, Chem. Phys. Lett. **435**, 119 (2007).
[18] K. Keem, H. Kim, G. T. Kim, J. S. Lee, B. Min, K. Cho, M. Y. Sung, and S. Kim, Appl. Phys. Lett. **84**, 4376 (2004).
[19] Z. Y. Fan, P. C. Chang, J. G. Lu, E. C. Walter, R. M. Penner, C. H. Lin, and H. P. Lee, Appl. Phys. Lett. **85**, 6128 (2004).
[20] C. Soci, A. Zhang, B. Xiang, S. A. Dayeh, D. P. R. Aplin, J. Park, X. Y. Bao, Y. H. Lo, and D. L. Wang, Nano Lett. **7**, 1003 (2007).
[21] H. Kind, H. Q. Yan, B. Messer, M. Law, and P. D. Yang, Adv. Mater. (Weinheim, Ger.) **14**, 158 (2002).
[22] S. Mathur, S. Barth, H. Shen, J. C. Pyun, and U. Werner, Small **1**, 713 (2005).
[23] O. Hayden, R. Agarwal, and C. M. Lieber, Nat. Mater. **5**, 352 (2006).
[24] S. M. Sze, *Physics of Semiconductor Devices* (Wiley, New York, 1981).
[25] C. S. Lao, Y. Li, C. P. Wong, and Z. L. Wang, Nano Lett. **7**, 1323 (2007).
[26] J. Liu, P. X. Gao, W. J. Mai, C. S. Lao, and Z. L. Wang, Appl. Phys. Lett. **89**, 063125 (2006).
[27] H. Jiang, J. T. Grant, K. Eyink, S. Tullis, J. Enlow, and T. J. Bunning, Polymer **46**, 8178 (2005).
[28] M. C. LeMieux, M. E. McConney, Y.-H. Lin, S. Singamaneni, H. Jiang, T. J. Bunning, and V. V. Tsukruk, Nano Lett. **6**, 730 (2006).
[29] B. K. An, S. K. Kwon, S. D. Jung, and S. Y. Park, J. Am. Chem. Soc. **124**, 14410 (2002).
[30] J. Jang, J. Bae, and E. Park, Adv. Funct. Mater. **16**, 1400 (2006).
[31] S. Singamaneni, M. C. LeMieux, H. Jiang, T. J. Bunning, and V. V. Tsukruk, Chem. Mater. **19**, 129 (2007).
[32] S. Pethkar, J. A. Dharmadhikari, A. A. Athawale, R. C. Aiyer, and K. Vijayamohanan, J. Phys. Chem. B **105**, 5110 (2001).
[33] J. J. Ge, H. Hou, Q. Li, M. J. Graham, A. Greiner, D. H. Reneker, F. W. Harris, and S. Z. D. Cheng, J. Am. Chem. Soc. **126**, 15754 (2004).
[34] M. C. Kim, S. H. Cho, J. G. Han, B. Y. Hong, Y. J. Kim, S. H. Yang, and J. H. Boo, Surf. Coat. Technol. **169**, 595 (2003).
[35] S. R. C. Vivekchand, K. C. Kam, G. Gundiah, A. Govindaraj, A. K. Cheetham, and C. N. R. Rao, J. Mater. Chem. **15**, 4922 (2005).